Physics Letters B 755 (2016) 403–408

Contents lists available at ScienceDirect

Physics Letters B

www.elsevier.com/locate/physletb

A resonance without resonance: Scrutinizing the diphoton excess at 750 GeV ☆

Jong Soo Kim [a], Jürgen Reuter [b], Krzysztof Rolbiecki [a,c,*], Roberto Ruiz de Austri [d]

[a] Instituto de Física Teórica, UAM/CSIC, Madrid, Spain
[b] DESY, Hamburg, Germany
[c] Institute of Theoretical Physics, University of Warsaw, Warsaw, Poland
[d] Instituto de Física Corpuscular, IFIC-UV/CSIC, Valencia, Spain

ARTICLE INFO

Article history:
Received 22 December 2015
Received in revised form 8 February 2016
Accepted 19 February 2016
Available online 24 February 2016
Editor: G.F. Giudice

Keywords:
BSM phenomenology
LHC

ABSTRACT

Motivated by the recent diphoton excesses reported by both ATLAS and CMS collaborations, we suggest that a new heavy spinless particle is produced in gluon fusion at the LHC and decays to a couple of lighter pseudoscalars which then decay to photons. The new resonances could arise from a new strongly interacting sector and couple to Standard Model gauge bosons only via the corresponding Wess–Zumino–Witten anomaly. We present a detailed recast of the newest 13 TeV data from ATLAS and CMS together with the 8 TeV data to scan the consistency of the parameter space for those resonances.

1. Introduction

After analyzing the first 13 TeV data, the ATLAS and CMS collaborations have reported an excess with respect to the background predictions in the diphoton channel search [1,2]. ATLAS has found the most significant deviation for a mass of about 750 GeV, corresponding to a local significance of 3.64σ using 3.3 fb^{-1} accumulated data, whereas CMS has a significance of 2.6σ for a mass about the same as ATLAS using 2.7 fb^{-1} data.

A simple explanation of such an excess could be through a resonance of a spin-0 or spin-2 particle with mass ~ 750 GeV that decays to photons [3–40], while spin-1 is excluded by the Yang–Landau theorem [41,42]. However, resonant production via the *s*-channel might be in tension with bounds imposed by run-I data [43–45]. This tension was quantified in e.g. [46]. Though a direct production of a resonance at 750 GeV and subsequent decay to two photons is not excluded, we propose an alternative scenario to explain the excess via a non-resonant process. We demonstrate our idea within the framework of strong dynamics around the TeV scale. The basis of the theoretical model is outlined in [47] (some of these ideas have also been mentioned in [3]) with the addition of two composite singlet scalar (or pseudoscalar) particles which couple to Standard Model (SM) gauge bosons via the Wess–Zumino–Witten anomaly [48,49], and to each other via a trilinear coupling. Here, we assume that the lighter 750 GeV pseudoscalar has no effective coupling to gluons and thus cannot be directly produced. Therefore, the lighter pseudoscalar has to be produced in the decay of the heavy one which can be produced via gluon fusion. In contrast to e.g. [3] we do not try to embed this into a complete model, but concentrate on the minimal simplified model that resembles a "composite sector toy model" including two resonances to describe the LHC results from the 8 and 13 TeV data sets.

The parameter space of the model then consists of the masses of the two (pseudo)scalar states, their decay constants, and their three operator coefficients to the field strengths of the three gauge groups of the SM. In this work we search for solutions that explain the excess, and to determine the best fit to the data by means of a numerical analysis.

This work is structured as follows. In Section 2 we present a general description of our model assumptions, whereas in Section 3 we describe the numerical procedure used to fit the data and show the results, and finally in Section 4 the conclusions are outlined.

2. Model assumptions

In this section, we describe in detail the assumptions for our simplified model setup to explain the ATLAS and CMS data. We discuss the most important phenomenological aspects of the sim-

☆ IFT-UAM/CSIC-15-137, DESY 15-255.

* Corresponding author at: Institute of Theoretical Physics, University of Warsaw, Warsaw, Poland.

E-mail addresses: jong.kim@csic.es (J.S. Kim), juergen.reuter@desy.de (J. Reuter), rolbiecki.krzysztof@csic.es (K. Rolbiecki), rruiz@ific.uv.es (R. Ruiz de Austri).

http://dx.doi.org/10.1016/j.physletb.2016.02.041

plified model below. Detailed information about the underlying assumptions on strongly interacting sectors for such a setup can be found e.g. in Refs. [3,47].

In our simplified model, we consider the SM particle spectrum extended by possible weak scale singlet spin 0 resonances. We assume that these new resonances (and possibly also the SM-like Higgs boson) are composite objects. However, the details of the electroweak symmetry breaking will not affect our numerical analysis and its results and thus we do not discuss it any further. We assume a hidden strongly interacting (confining) gauge group G_N. Two pseudoscalar resonances σ and η emerge as the Nambu Goldstone bosons of the broken gauge group G_N.[1] The kinetic terms of the weak singlet pseudoscalars are given by

$$\mathcal{L}_{\text{kin}} = \frac{1}{2}\partial_\mu\eta\partial^\mu\eta + \frac{1}{2}\partial_\mu\sigma\,\partial^\mu\sigma - \frac{1}{2}m_\eta^2\eta^2 - \frac{1}{2}m_\sigma^2\sigma^2\,. \tag{1}$$

Here, m_η and m_σ are the mass terms of the real pseudoscalar fields η and σ. We assume the following parity violating trilinear σ–η–η interaction term,[2]

$$\mathcal{L}_{\text{trilinear}} = \lambda\,\sigma\,\eta\eta\,, \tag{2}$$

where λ is a real parameter of mass dimension one. In a more general framework, all interaction terms up to mass dimension 4 consistent with our model should be included. However, since the diphoton excess can be explained with the trilinear interaction term only, we will omit these terms in the remainder of the letter. Note that such a term is the simplest assumption one can make about such a trilinear coupling. This kind of coupling arises e.g. in the form of a scalar–pseudoscalar–pseudoscalar coupling, $\Phi\eta\eta$, in certain types of Little Higgs models [50,51]. These are variants of composite models, endowed with a certain symmetry structure. Similar mechanisms can generate such couplings also in plain composite models. Introducing explicit CP violation into symmetry-breaking terms of the non-linear sector will correspondingly generate couplings of the type of Eq. (2).

Alternatively, such couplings could arise with a different Lorentz structure using chiral perturbation theory for composite models as [52,53]

$$\begin{aligned}&\mathcal{L} = \text{tr}\left[\partial_\mu U\partial^\mu U^\dagger\left(MU + U^\dagger M\right)\right]\\ \Longrightarrow\ &\mathcal{L}'_{\text{trilinear}} = \lambda'\,\sigma\,(\partial_\mu\eta\partial^\mu\eta)\,.\end{aligned} \tag{3}$$

Here, U is the Goldstone boson non-linear field matrix, and M is a mass matrix for the underlying, condensing new fermions. Though this leads to a different Lorentz structure, for the signal rate arguments used in this paper, it does not change the conclusions.

The new resonances only couple to the SM gauge bosons via the Wess–Zumino–Witten (WZW) anomaly [48,49],

$$\mathcal{L}_{\phi gg} = \kappa_g^\phi\frac{g_3^2}{32\pi^2}\frac{1}{F_\phi}\epsilon^{\mu\nu\rho\sigma}G^a_{\mu\nu}G^a_{\rho\sigma}\phi, \tag{4}$$

$$\mathcal{L}_{\phi WW} = \kappa_W^\phi\frac{g_2^2}{32\pi^2}\frac{1}{F_\phi}\epsilon^{\mu\nu\rho\sigma}W^i_{\mu\nu}W^i_{\rho\sigma}\phi, \tag{5}$$

$$\mathcal{L}_{\phi BB} = \kappa_B^\phi\frac{g_Y^2}{32\pi^2}\frac{1}{F_\phi}\epsilon^{\mu\nu\rho\sigma}B_{\mu\nu}B_{\rho\sigma}\phi, \tag{6}$$

[1] There are possibly more resonances, but they do not play a role for the moment as no further signals have been observed yet.

[2] We assume that parity is explicitly violated via a nonzero θ term in the gauge group G_N. In principle, the heavier resonance σ could also be scalar, without the need for CP violation in this interaction. However, then it needs to be a glueball in the confining theory which is difficult to justify why it should be so much heavier then the η [47].

Table 1
Selection cuts of the 13 TeV ATLAS/CMS diphoton searches [1,2].

ATLAS	CMS
$p_T(\gamma) \geq 25$ GeV	$p_T(\gamma) \geq 75$ GeV
$\lvert\eta^\gamma\rvert \leq 2.37$	$\lvert\eta^\gamma\rvert \leq 1.44$ or $1.57 \leq \lvert\eta^\gamma\rvert \leq 2.5$ at least one γ with $\lvert\eta^\gamma\rvert \leq 1.44$
$E_T^{\gamma_1}/m_{\gamma\gamma} \geq 0.4$, $E_T^{\gamma_2}/m_{\gamma\gamma} \geq 0.3$	$m_{\gamma\gamma} \geq 230$ GeV

with $\phi = \eta$ or σ. Here, κ_i^η, κ_i^σ and F_η, F_σ denote arbitrary real coefficients and pseudoscalar decay constants, respectively. $G_{\mu\nu}$, $W_{\mu\nu}$ and $B_{\mu\nu}$ are the color, weak isospin and abelian hypercharge field strength, and g_3, g_2 and g_Y denote the corresponding dimensionless SM gauge couplings. The prefactors κ_i^η and κ_i^σ can be explicitly calculated in a complete model, i.e. if the particle content (fermions in the composite sector and their exact quantum numbers) in the triangle loop is known [3,47]. However, in this work we do not consider a particular model and assume that the coefficients κ_i^η and κ_i^σ are free parameters of our effective Lagrangian. In the following, we will assume that the coefficients are independent and determine their values in a numerical analysis without referring to a specific model. A possible realization of the phenomenological model discussed here will be presented below at the end of the section.

In this paper, we assume that the 750 GeV resonance is not directly produced via s channel, as this has already been studied in the literature, and there is this tension with constraints from Run 1 data. In order to accomplish indirect production, we set the corresponding anomaly coefficient to zero, $\kappa_g^\eta = 0$. So its production must occur via the heavy resonance σ assuming that σ has anomaly induced couplings to the gluons. Thus, we consider a hierarchical scenario in order to evade the 8 TeV limits. We focus on resonant production of the heavy singlet pseudoscalar σ via gluon fusion with subsequent on-shell decay into a pair of η's. The light pseudoscalar η is allowed to decay into all electroweak SM gauge bosons via the WZW mechanism (but at least photons and Z, which is inevitable). Thus, we expect the following signature

$$pp \to \sigma \to \eta\eta \to \gamma\gamma + X, \tag{7}$$

where X denotes the rest of the event. Both experiments, ATLAS and CMS do not veto on X. We have listed the selection cuts from ATLAS and CMS in Table 1. Hence, this signature can explain the diphoton excess. The anomaly coefficients for the weak and hypercharge group have been partially set to zero as they are phenomenologically not relevant for the numerical analysis (in the case of the heavy resonance), or are not allowed in order not to give a too small branching fraction into photons (for the light resonance). Note that there is a certain redundancy of parameters in the simplified model, as changes to the decay constant can within a certain range of parameters always be emulated by changes in the anomaly coefficient.[3]

Our choice of anomaly coefficients resembles the following composite model which was discussed in Ref. [3]. Here, two vector-like fermions Q_1 and Q_2 are introduced. Both vector-like fermions are in the fundamental representation of the strong gauge group G_N with a dynamical scale Λ. Here, we identify G_N with an asymptotically free SU(N) gauge theory. The charge assignments of Q_1 and Q_2 under $SU(N) \times \text{SU}(3)_C \times \text{SU}(2)_L \times \text{U}(1)_Y$ are $(N, 1, 2, a)$ and $(N, \bar{3}, 1, b)$, respectively. N denotes the fundamental represen-

[3] Note that our setup in principle also includes glueballs of the composite theory where, however, the decomposition of the operator coefficients into dimensionful parameters would be different due to a different power counting.

Table 2
Variable input parameters of our pseudoscalar scenario and the range over which these parameters are scanned to find the best fit point solution.

Parameter	Description	Value or range
m_σ	mass of heavier resonance	[1.5 TeV, 2.5 TeV]
m_η	mass of lighter resonance	750 GeV
λ	dimensionful $\eta\sigma\sigma$	[0. TeV, 1.5 TeV]
F_η	η decay constant	1 TeV
F_σ	σ decay constant	1 TeV
κ_g^η	anomaly coefficient	0
κ_W^η	anomaly coefficient	0
κ_B^η	anomaly coefficient	1
κ_g^σ	anomaly coefficient	[0, 15]
κ_W^σ	anomaly coefficient	0
κ_B^σ	anomaly coefficient	0

tation of the $SU(N)$. Now, we assume that $m_1 < \Lambda < m_2$. At low energies, we have the following condensate

$$\eta \sim \langle Q_1 \bar{Q}_1 \rangle, \tag{8}$$

where η is a triplet under $SU(2)_L$. The only allowed anomaly induced coupling of η is given by the following term

$$\mathcal{L} \propto \eta^b W^{b\mu\nu} \tilde{B}_{\mu\nu}. \tag{9}$$

Since the (pseudo)scalar η^b cannot couple to gluons, it cannot be produced directly. However, heavy resonances with Q_1 pairs can be produced which then decay into the lighter pseudoscalar via Eq. (2). The latter can then decay to two photons. Using more than two underlying fundamental fermions of the confining gauge group $SU(N)$ with appropriate quantum numbers, more general scenarios can be constructed.

3. Numerical results

In the following, we first briefly discuss the numerical tools and then describe our numerical framework. Finally, we will discuss our results.

3.1. Numerical tools

We have implemented the model discussed in Section 2 with the program `FeynRules 2.3.13` [54] and created a `UFO` output [55] for the numerical studies. Parton level events were generated with `Madgraph 2.3.3` [56] interfaced with `Pythia 6.4` [57] for the parton shower and hadronization. Branching ratios and cross sections have been cross-checked with an independent numerical implementation of the simplified model into `WHIZARD 2.2.8` [58–60]. We have implemented the 8 and 13 TeV diphoton searches from ATLAS and CMS [1,2] into the `CheckMATE 1.2.2` framework [61] with its `AnalysisManager` [62]. `CheckMATE 1.2.2` is based on the fast detector simulation `Delphes 3.10` [63] with heavily modified detector tunes and it determines the number of expected signal events passing the selection cuts of the particular analysis. The selection cuts for both ATLAS and CMS analyses are shown in Table 1.

3.2. Scan procedure

In order to find values of parameters that provide a good description of data we performed a scan in λ, κ_g^σ and the mass of heavier resonance, m_σ, in the ranges displayed in Table 2. We simulated pair production of η states via resonant s-channel σ exchange.[4] All decay modes of η were included in the simulation. For each point the number of events passing experimental selections in our simulation is compared to the number of events reported by the LHC collaborations, see Table 3. The expected number of background events is extracted from the respective publication. Because the experiments did not clearly define signal regions, we performed a fit in the invariant mass window $700 < m_{\gamma\gamma} < 800$ GeV. For the CMS search we split the events into the barrel (EBEB) and end-cap (EBEE) regions, following the collaboration's procedure. Finally, the 8 TeV searches are used solely as a consistency check in order to see if the parameter points were not excluded during the previous run.

Table 3
The number of events for each of the signal regions: observed, SM background, our 'best fit' according to the simulation results and the $\Delta\chi^2$ contribution. 'EBEB' denotes the signal region with both photons in the barrel while 'EBEE' the signal region with one photon in the end-cap. 'Best fit' point input: $\lambda = 0.22$ TeV, $\kappa_g^\sigma = 4.3$, $m_\sigma = 1.75$ TeV.

Signal region	Observed	Background	Best fit	$\Delta\chi^2$
ATLAS	28	11.4 ± 3	12.0	0.56
CMS EBEB	14	9.5 ± 1.9	8.1	0.74
CMS EBEE	16	18.5 ± 3.7	1.3	0.48

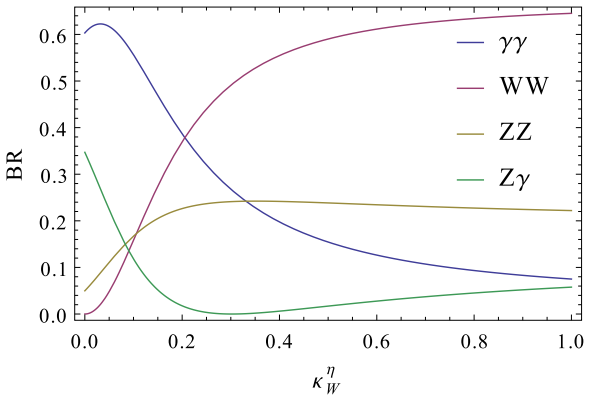

Fig. 1. The branching ratios for the decays of η as a function of κ_W^η with $\kappa_B^\eta = 1$.

Clearly, the pseudoscalar sector is parametrized by several *a priori* free parameters, as can be seen in Table 2. For simplicity, in the current analysis we set some of them to zero, therefore our heavy pseudoscalar couples only to gluons through the anomaly while the light one only to B. The light pseudoscalar will still have other decay modes to ZZ and $Z\gamma$. Once the κ_W^η coupling is allowed, additional decay modes to WW pairs will be open. We show the decay pattern of η in Fig. 1. This will provide a distinctive feature at colliders: the diphoton pairs will be often accompanied by jets, leptons or missing transverse energy. Depending on the actual mass hierarchy between scalars, the $\gamma\gamma$ pair can have a significant transverse momentum, which will eventually vanish close to the threshold for the decay $\sigma \to \eta\eta$. This feature together with an additional activity in the event can serve as a way to probe this type of models soon.[5]

The fit was performed with the χ^2 test statistics. Namely,

$$\chi_i^2 = \frac{(n_i - \mu_i)^2}{\sigma_{i,\text{stat}}^2 + \sigma_{i,b}^2}, \tag{10}$$

[4] This neglects possible box diagram contributions to η pair production which, however, are equal to zero if the QCD WZW anomaly of the η current vanishes.

[5] We note that according to the CMS speaker's statement during the seminar presenting those results at CERN, no difference between the peak and side-band regions was observed. Given the low number of events and lack of details in the conference note [2] we do not take this remark as conclusive.

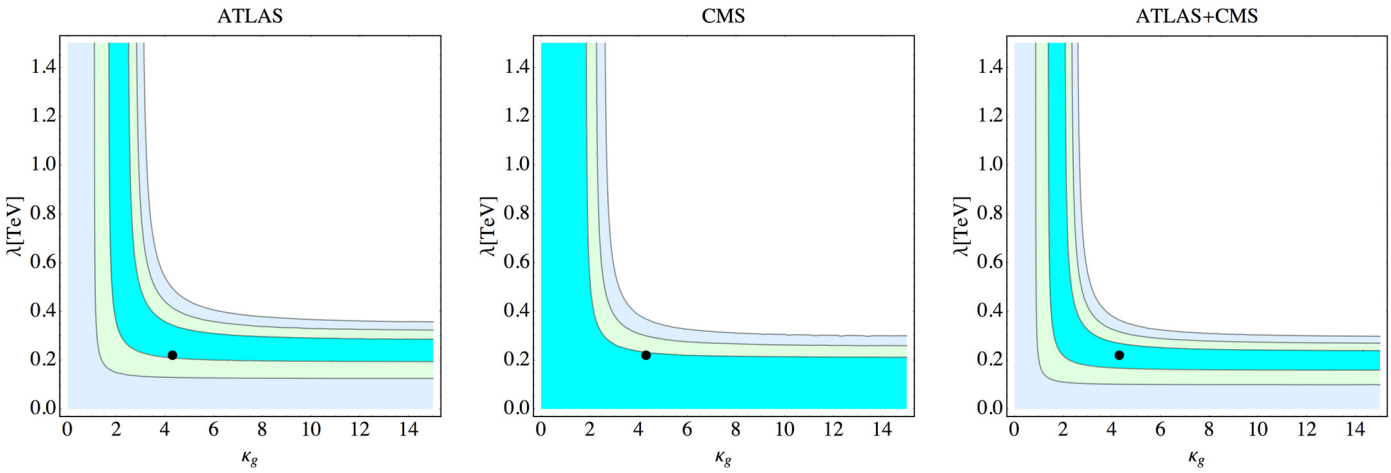

Fig. 2. The distribution of the χ^2 test as a function of the dimensionful coupling κ_g^σ and λ for ATLAS [1], CMS [2] and both experiments combined with m_σ set to 1.75 TeV. The colors and contours denote: cyan $\Delta\chi^2 = 1$ above minimum; light green $\Delta\chi^2 = 4$ above minimum; and light blue $\Delta\chi^2 = 9$ above minimum. The dots represent sample best-fit point: $\lambda = 0.22$ TeV, $\kappa_g^\sigma = 4.3$, $m_\sigma = 1.75$ TeV. (For interpretation of the references to color in this figure legend, the reader is referred to the web version of this article.)

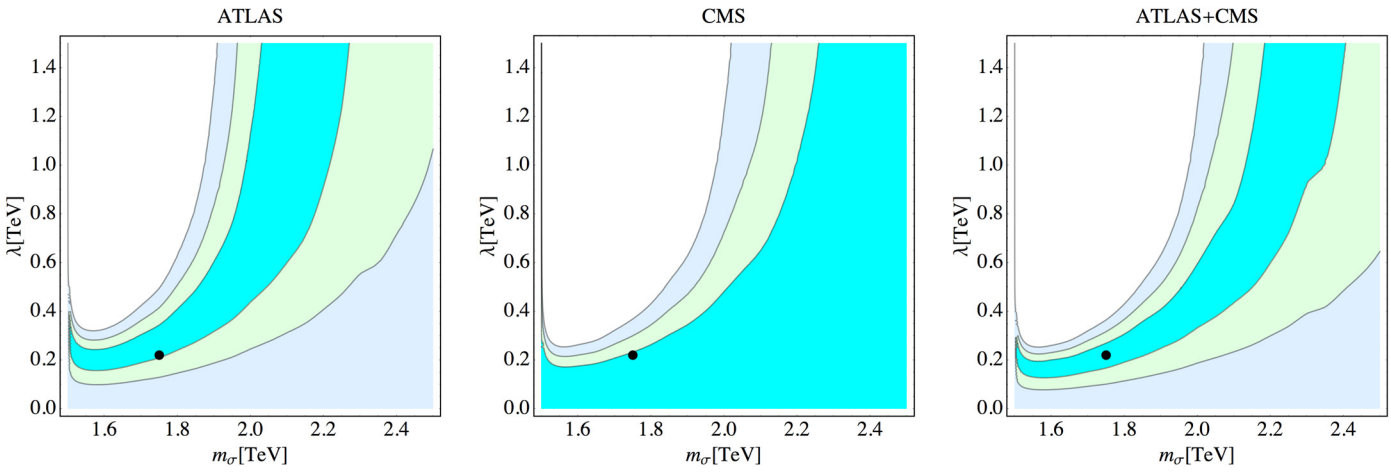

Fig. 3. The distribution of the χ^2 test as a function of the dimensionful coupling m_σ and λ for ATLAS [1], CMS [2] and both experiments combined with κ_g^σ set to 4.3. The colors and contours denote: cyan $\Delta\chi^2 = 1$ above minimum; light green $\Delta\chi^2 = 4$ above minimum; and light blue $\Delta\chi^2 = 9$ above minimum. The dots represent the sample best-fit point: $\lambda = 0.22$ TeV, $\kappa_g^\sigma = 4.3$, $m_\sigma = 1.75$ TeV. (For interpretation of the references to color in this figure legend, the reader is referred to the web version of this article.)

where

$$\mu_i = \mu_{i,b} + \mu_{i,s}\,. \tag{11}$$

Here, n_i is the number of observed events, $\mu_{i,b}$ is the expected number of background events, $\mu_{i,s}$ is the expected number of signal events, $\sigma_{i,\text{stat}}$ and $\sigma_{i,b}$ are the statistical and systematic uncertainty on the expected number of background events for each signal region, where the index i runs over the i = ATLAS, CMS EBEB, CMS EBEE selections. The systematic errors combine the experimental ones as given by the collaborations and additionally 10% error on the CheckMATE event yield. In any case, the total error is dominated by the statistical errors due to the low number of events. We assume that all errors are uncorrelated. The signal regions are defined as $700 < m_{\gamma\gamma} < 800$ GeV.

3.3. Discussion

As explained above, we have performed a scan as a function of the couplings λ, κ_g^σ and the mass m_σ while keeping the other parameters fixed as it is shown in Table 2. This has been done with the ATLAS and CMS searches and in the following we combine the data of both experiments.

Fig. 2 shows the χ^2 as a function of κ_g^σ and λ (left panel for ATLAS data alone, middle panel for CMS data alone and right panel for their combination). The contours are plotted for $\Delta\chi^2 = 1, 4, 9$ above minimum respectively. It is interesting to notice that the χ^2 follows a hyperbolic shape in the λ, κ_g^σ plane since as it is expected there is a degeneracy among the two couplings. Namely an increase in the κ_g^σ coupling enhances the production rate of the σ field via gluon-fusion which is compensated by a decrease of the λ coupling which affects the decay branching fraction of σ decaying to a pair of η's. The black dots represent one of the low χ^2 points: $\lambda = 0.22$ TeV, $\kappa_g^\sigma = 4.3$, $m_\sigma = 1.75$ TeV.

Fig. 3 shows the χ^2 as a function of m_σ and λ (again, left panel for ATLAS data alone, middle panel for CMS data alone and right panel for their combination). The contours are plotted for $\Delta\chi^2 = 1, 4, 9$ above minimum respectively. Finally, Fig. 4 shows the χ^2 as a function of κ_g^σ and m_σ, with the black dot defined as above. The preferred values of parameters lie close to the border of 1-σ for each of the experiments. Clearly CMS is more consistent with the no signal hypothesis, while ATLAS prefers higher event yields.

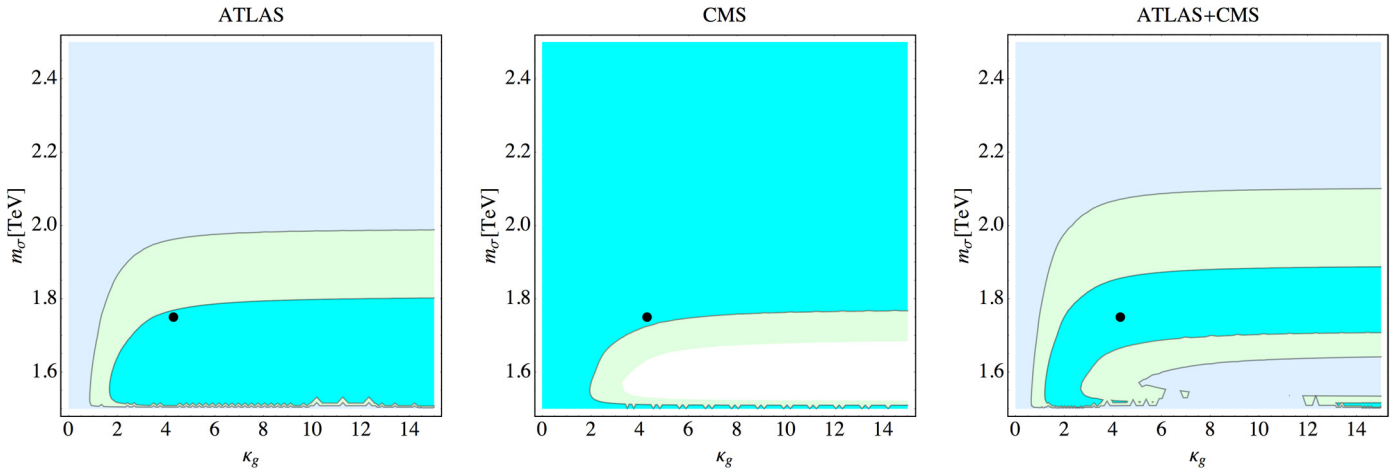

Fig. 4. The distribution of the χ^2 test as a function of the dimensionful coupling κ_g^σ and m_σ for ATLAS [1], CMS [2] and both experiments combined with λ set to 0.22 TeV. The colors and contours denote: cyan $\Delta\chi^2 = 1$ above minimum; light green $\Delta\chi^2 = 4$ above minimum; and light blue $\Delta\chi^2 = 9$ above minimum. The dots represent the sample best-fit point: $\lambda = 0.22$ TeV, $\kappa_g^\sigma = 4.3$, $m_\sigma = 1.75$ TeV. (For interpretation of the references to color in this figure legend, the reader is referred to the web version of this article.)

Because we effectively only have one observable it is not surprising that there is a continuum of points with minimum χ^2 value. The combined analysis gives the χ^2 value at the minimum of 1.8. This should be compared to the SM-only hypothesis which yields $\chi^2_{\rm SM} = 8.8$. Finally, we provide the expected and observed numbers of events for each signal region in Table 3.

As already mentioned, because we effectively have one observable the degeneracy in the preferred parameters cannot be resolved at this point. The degeneracy could be broken by an observation of a peak in the dijet mass spectra from the decay $\sigma \to gg$. Since in the range of masses m_σ studied here the results are consistent with the background-only hypothesis [64,65], one should also take into account an additional constraint from these searches. CMS [64] provides explicit limits for the digluon final state. For our sample point at $m_\sigma = 1.75$ TeV, the upper limit on the visible dijet cross section is 1.8 pb. Taking into account the efficiency of 60% the truth cross section should be less than ~ 3 pb. This implies $\kappa_g^\sigma \lesssim 25$.

Finally, we comment on the visibility of the diphoton signal at 8 TeV [43–45,66]. The cross section, assuming the gluon–gluon production mode [67], would be a factor 15 smaller. On the other hand, the luminosity recorded at 8 TeV was some 6 times larger than at 13 TeV in case of ATLAS. For the sample point from Table 3 the expected event yield would be 4.8 events in the ATLAS search [44], while the observed (expected) 95% CL upper limit is 23.1 (21.9). Similarly, in the CMS case we find the 8 TeV constraints easily fulfilled.

4. Conclusions

In this work we present a model based on composite states that fits well the diphoton excess observed by the ATLAS and CMS collaborations which points to the existence of a resonance of mass of about 750 GeV.

The mechanism consists in the production of a heavy pseudoscalar via gluon fusion with a mass in a range 1.5–2.5 TeV, which decays to a pair of lighter pseudoscalars with a mass of about 750 GeV that finally decay to photons. While both pseudoscalars couple to the SM gauge bosons via the WZW anomaly, the heavy pseudoscalar couples to the light ones via a dimensionful trilinear coupling which is allowed by the theory.

We find a specific direction in the parameter space of the simplified model that minimizes χ^2 from the combined analysis of the ATLAS and CMS data at the value of 1.8 and the model markedly improves the SM-only value of 8.8. It is also consistent with the 8 TeV searches. Its distinctive feature in the collider experiments compared to the direct s-channel resonance would be a non-trivial p_T spectrum of the diphoton pairs and the presence of additional jets, leptons or missing energy, depending on the decays of gauge bosons produced in the opposite decay chain, which makes it easily testable with more data from the upcoming run.

Acknowledgements

We would like to thank Sascha Caron for useful discussions. R.R.d.A. is supported by the Ramón y Cajal program of the Spanish MICINN and also thanks for the support of the Spanish MICINN's Consolider-Ingenio 2010 Programme under the grant MULTIDARK CSD2209-00064, the Invisibles European ITN project (FP7-PEOPLE-2011-ITN, PITN-GA-2011-289442-INVISIBLES) and the "SOM Sabor y origen de la Materia" (FPA2011-29678) and the "Fenomenologia y Cosmologia de la Fisica mas alla del Modelo Estandar e Implicaciones Experimentales en la era del LHC" (FPA2010-17747) MEC projects. K.R. and J.S.K. have been partially supported by the MINECO (Spain) under contract FPA2013-44773-P; Consolider-Ingenio CPAN CSD2007-00042; the Spanish MINECO Centro de excelencia Severo Ochoa Program under grant SEV-2012-0249; and by JAE-Doc program. J.R. wants to thank for the hospitality at the IFT of the Universidad Autonoma de Madrid, where this work has been initiated.

References

[1] ATLAS Collaboration, Search for resonances decaying to photon pairs in 3.2 inverse fb of p p collisions at $\sqrt{s} = 13$ TeV with the ATLAS detector, ATLAS-CONF-2015-081.
[2] CMS Collaboration, Search for new physics in high mass diphoton events in proton–proton collisions at 13 TeV, CMS PAS EXO-15-004.
[3] K. Harigaya, Y. Nomura, Composite models for the 750 GeV diphoton excess, arXiv:1512.04850 [hep-ph].
[4] Y. Mambrini, G. Arcadi, A. Djouadi, The LHC diphoton resonance and dark matter, arXiv:1512.04913 [hep-ph].
[5] M. Backovic, A. Mariotti, D. Redigolo, Di-photon excess illuminates dark matter, arXiv:1512.04917 [hep-ph].
[6] A. Angelescu, A. Djouadi, G. Moreau, Scenarii for interpretations of the LHC diphoton excess: two Higgs doublets and vector-like quarks and leptons, arXiv:1512.04921 [hep-ph].
[7] D. Buttazzo, A. Greljo, D. Marzocca, Knocking on new physics' door with a scalar resonance, arXiv:1512.04929 [hep-ph].

[8] S. Knapen, T. Melia, M. Papucci, K. Zurek, Rays of light from the LHC, arXiv:1512.04928 [hep-ph].
[9] Y. Nakai, R. Sato, K. Tobioka, Footprints of new strong dynamics via anomaly, arXiv:1512.04924 [hep-ph].
[10] A. Pilaftsis, Diphoton signatures from heavy axion decays at LHC, arXiv:1512.04931 [hep-ph].
[11] R. Franceschini, G.F. Giudice, J.F. Kamenik, M. McCullough, A. Pomarol, R. Rattazzi, M. Redi, F. Riva, A. Strumia, R. Torre, What is the gamma gamma resonance at 750 GeV?, arXiv:1512.04933 [hep-ph].
[12] S. Di Chiara, L. Marzola, M. Raidal, First interpretation of the 750 GeV di-photon resonance at the LHC, arXiv:1512.04939 [hep-ph].
[13] T. Higaki, K.S. Jeong, N. Kitajima, F. Takahashi, The QCD axion from aligned axions and diphoton excess, arXiv:1512.05295 [hep-ph].
[14] S.D. McDermott, P. Meade, H. Ramani, Singlet scalar resonances and the diphoton excess, arXiv:1512.05326 [hep-ph].
[15] J. Ellis, S.A.R. Ellis, J. Quevillon, V. Sanz, T. You, On the interpretation of a possible ~ 750 GeV particle decaying into $\gamma\gamma$, arXiv:1512.05327 [hep-ph].
[16] M. Low, A. Tesi, L.-T. Wang, A pseudoscalar decaying to photon pairs in the early LHC run 2 data, arXiv:1512.05328 [hep-ph].
[17] B. Bellazzini, R. Franceschini, F. Sala, J. Serra, Goldstones in diphotons, arXiv:1512.05330 [hep-ph].
[18] R.S. Gupta, S. Jaeger, Y. Kats, G. Perez, E. Stamou, Interpreting a 750 GeV diphoton resonance, arXiv:1512.05332 [hep-ph].
[19] C. Petersson, R. Torre, The 750 GeV diphoton excess from the goldstino superpartner, arXiv:1512.05333 [hep-ph].
[20] E. Molinaro, F. Sannino, N. Vignaroli, Strong dynamics or axion origin of the diphoton excess, arXiv:1512.05334 [hep-ph].
[21] B. Dutta, Y. Gao, T. Ghosh, I. Gogoladze, T. Li, Interpretation of the diphoton excess at CMS and ATLAS, arXiv:1512.05439 [hep-ph].
[22] Q.-H. Cao, Y. Liu, K.-P. Xie, B. Yan, D.-M. Zhang, A boost test of anomalous diphoton resonance at the LHC, arXiv:1512.05542 [hep-ph].
[23] S. Matsuzaki, K. Yamawaki, 750 GeV diphoton signal from one-family walking technipion, arXiv:1512.05564 [hep-ph].
[24] A. Kobakhidze, F. Wang, L. Wu, J.M. Yang, M. Zhang, LHC diphoton excess explained as a heavy scalar in top-seesaw model, arXiv:1512.05585 [hep-ph].
[25] R. Martinez, F. Ochoa, C.F. Sierra, Diphoton decay for a 750 GeV scalar dark matter, arXiv:1512.05617 [hep-ph].
[26] P. Cox, A.D. Medina, T.S. Ray, A. Spray, Diphoton excess at 750 GeV from a radion in the bulk-Higgs scenario, arXiv:1512.05618 [hep-ph].
[27] D. Becirevic, E. Bertuzzo, O. Sumensari, R.Z. Funchal, Can the new resonance at LHC be a CP-odd Higgs boson?, arXiv:1512.05623 [hep-ph].
[28] J.M. No, V. Sanz, J. Setford, See-saw composite Higgses at the LHC: linking naturalness to the 750 GeV di-photon resonance, arXiv:1512.05700 [hep-ph].
[29] S.V. Demidov, D.S. Gorbunov, On sgoldstino interpretation of the diphoton excess, arXiv:1512.05723 [hep-ph].
[30] W. Chao, R. Huo, J.-H. Yu, The minimal scalar-stealth top interpretation of the diphoton excess, arXiv:1512.05738 [hep-ph].
[31] S. Fichet, G. von Gersdorff, C. Royon, Scattering light by light at 750 GeV at the LHC, arXiv:1512.05751 [hep-ph].
[32] D. Curtin, C.B. Verhaaren, Quirky explanations for the diphoton excess, arXiv:1512.05753 [hep-ph].
[33] L. Bian, N. Chen, D. Liu, J. Shu, A hidden confining world on the 750 GeV diphoton excess, arXiv:1512.05759 [hep-ph].
[34] J. Chakrabortty, A. Choudhury, P. Ghosh, S. Mondal, T. Srivastava, Di-photon resonance around 750 GeV: shedding light on the theory underneath, arXiv:1512.05767 [hep-ph].
[35] A. Ahmed, B.M. Dillon, B. Grzadkowski, J.F. Gunion, Y. Jiang, Higgs-radion interpretation of 750 GeV di-photon excess at the LHC, arXiv:1512.05771 [hep-ph].
[36] P. Agrawal, J. Fan, B. Heidenreich, M. Reece, M. Strassler, Experimental considerations motivated by the diphoton excess at the LHC, arXiv:1512.05775 [hep-ph].
[37] C. Csaki, J. Hubisz, J. Terning, The minimal model of a diphoton resonance: production without gluon couplings, arXiv:1512.05776 [hep-ph].
[38] A. Falkowski, O. Slone, T. Volansky, Phenomenology of a 750 GeV singlet, arXiv:1512.05777 [hep-ph].
[39] D. Aloni, K. Blum, A. Dery, A. Efrati, Y. Nir, On a possible large width 750 GeV diphoton resonance at ATLAS and CMS, arXiv:1512.05778 [hep-ph].
[40] Y. Bai, J. Berger, R. Lu, A 750 GeV dark pion: cousin of a dark G-parity-odd WIMP, arXiv:1512.05779 [hep-ph].
[41] L.D. Landau, On the angular momentum of a system of two photons, Dokl. Akad. Nauk Ser. Fiz. 60 (2) (1948) 207–209.
[42] C.-N. Yang, Selection rules for the dematerialization of a particle into two photons, Phys. Rev. 77 (1950) 242–245.
[43] ATLAS Collaboration, G. Aad, et al., Search for scalar diphoton resonances in the mass range 65–600 GeV with the ATLAS detector in pp collision data at $\sqrt{s} = 8$ TeV, Phys. Rev. Lett. 113 (17) (2014) 171801, arXiv:1407.6583 [hep-ex].
[44] ATLAS Collaboration, G. Aad, et al., Search for high-mass diphoton resonances in pp collisions at $\sqrt{s} = 8$ TeV with the ATLAS detector, Phys. Rev. D 92 (3) (2015) 032004, arXiv:1504.05511 [hep-ex].
[45] CMS Collaboration, V. Khachatryan, et al., Search for diphoton resonances in the mass range from 150 to 850 GeV in pp collisions at $\sqrt{s} = 8$ TeV, Phys. Lett. B 750 (2015) 494–519, arXiv:1506.02301 [hep-ex].
[46] J.S. Kim, K. Rolbiecki, R.R. de Austri, Model-independent combination of diphoton constraints at 750 GeV, arXiv:1512.06797 [hep-ph].
[47] G. Cacciapaglia, A. Deandrea, M. Hashimoto, Scalar hint from the diboson excess?, Phys. Rev. Lett. 115 (17) (2015) 171802, arXiv:1507.03098 [hep-ph].
[48] J. Wess, B. Zumino, Consequences of anomalous Ward identities, Phys. Lett. B 37 (1971) 95.
[49] E. Witten, Global aspects of current algebra, Nucl. Phys. B 223 (1983) 422–432.
[50] W. Kilian, D. Rainwater, J. Reuter, Pseudo-axions in little Higgs models, Phys. Rev. D 71 (2005) 015008, arXiv:hep-ph/0411213.
[51] W. Kilian, D. Rainwater, J. Reuter, Distinguishing little-Higgs product and simple group models at the LHC and ILC, Phys. Rev. D 74 (2006) 095003, arXiv:hep-ph/0609119;
W. Kilian, D. Rainwater, J. Reuter, Distinguishing little-Higgs product and simple group models at the LHC and ILC, Phys. Rev. D 74 (2006) 099905 (Erratum).
[52] J. Gasser, H. Leutwyler, Chiral perturbation theory to one loop, Ann. Phys. 158 (1984) 142.
[53] J. Gasser, H. Leutwyler, Chiral perturbation theory: expansions in the mass of the strange quark, Nucl. Phys. B 250 (1985) 465.
[54] A. Alloul, N.D. Christensen, C. Degrande, C. Duhr, B. Fuks, FeynRules 2.0 – a complete toolbox for tree-level phenomenology, Comput. Phys. Commun. 185 (2014) 2250–2300, arXiv:1310.1921 [hep-ph].
[55] C. Degrande, C. Duhr, B. Fuks, D. Grellscheid, O. Mattelaer, T. Reiter, UFO – the universal FeynRules output, Comput. Phys. Commun. 183 (2012) 1201–1214, arXiv:1108.2040 [hep-ph].
[56] J. Alwall, R. Frederix, S. Frixione, V. Hirschi, F. Maltoni, O. Mattelaer, H.S. Shao, T. Stelzer, P. Torrielli, M. Zaro, The automated computation of tree-level and next-to-leading order differential cross sections, and their matching to parton shower simulations, J. High Energy Phys. 07 (2014) 079, arXiv:1405.0301 [hep-ph].
[57] T. Sjostrand, S. Mrenna, P.Z. Skands, PYTHIA 6.4 physics and manual, J. High Energy Phys. 05 (2006) 026, arXiv:hep-ph/0603175.
[58] W. Kilian, T. Ohl, J. Reuter, WHIZARD: simulating multi-particle processes at LHC and ILC, Eur. Phys. J. C 71 (2011) 1742, arXiv:0708.4233 [hep-ph].
[59] M. Moretti, T. Ohl, J. Reuter, O'Mega: an optimizing matrix element generator, arXiv:hep-ph/0102195.
[60] N.D. Christensen, C. Duhr, B. Fuks, J. Reuter, C. Speckner, Introducing an interface between WHIZARD and FeynRules, Eur. Phys. J. C 72 (2012) 1990, arXiv:1010.3251 [hep-ph].
[61] M. Drees, H. Dreiner, D. Schmeier, J. Tattersall, J.S. Kim, CheckMATE: confronting your favourite new physics model with LHC data, Comput. Phys. Commun. 187 (2014) 227–265, arXiv:1312.2591 [hep-ph].
[62] J.S. Kim, D. Schmeier, J. Tattersall, K. Rolbiecki, A framework to create customised LHC analyses within CheckMATE, Comput. Phys. Commun. 196 (2015) 535–562, arXiv:1503.01123 [hep-ph].
[63] DELPHES 3 Collaboration, J. de Favereau, C. Delaere, P. Demin, A. Giammanco, V. Lemaître, A. Mertens, M. Selvaggi, DELPHES 3, a modular framework for fast simulation of a generic collider experiment, J. High Energy Phys. 02 (2014) 057, arXiv:1307.6346 [hep-ex].
[64] CMS Collaboration, V. Khachatryan, et al., Search for narrow resonances decaying to dijets in proton–proton collisions at sqrt(s) = 13 TeV, arXiv:1512.01224 [hep-ex].
[65] ATLAS Collaboration, G. Aad, et al., Search for new phenomena in dijet mass and angular distributions from pp collisions at $\sqrt{s} = 13$ TeV with the ATLAS detector, arXiv:1512.01530 [hep-ex].
[66] CMS Collaboration, Search for high-mass diphoton resonances in pp collisions at sqrt(s) = 8 TeV with the CMS detector, Tech. Rep. CMS-PAS-EXO-12-045, CERN, Geneva, 2015, https://cds.cern.ch/record/2017806.
[67] LHCSWG, LHC Higgs cross section working group, https://twiki.cern.ch/twiki/bin/view/LHCPhysics/CrossSections.